International Council for the Exploration of the Sea

ICES CM 2006/I:22

Correcting for avoidance in acoustic abundance estimates for herring using a generalized linear model

Vidar Hjellvik, Nils Olav Handegard and Egil Ona

Abstract

When a research vessel passes over a herring school or layer, the herring may avoid the vessel by swimming downwards and horizontally. The fish may also change its orientation, which may alter its mean target strength. Consequently, the echo abundance measured by the relatively narrow echo sounder beam does not always reflect the true density of the school. The fish reaction is strongest in the upper parts of the water column. This avoidance behaviour has been quantified in several experiments where a stationary, submerged transducer has been used to measure the changes in echo abundance during the passage of a survey vessel. In this paper two approaches for correcting the echo abundance for avoidance are investigated. The first approach is to correct the echo abundance in each depth layer separately; the second is to correct the total echo abundance, letting the correction depend on the mean depth of the fish at passing. In both approaches generalized linear models are fitted to the experimental data. Since the parameters are estimated with uncertainty, this uncertainty can be taken into account when the fitted models are used for correcting standard survey data.

Keywords: Acoustics, uncertainty, avoidance, correction, generalized linear models

Contact author:

Vidar Hjellvik: Institute of Marine Research, P.O. Box 1870 Nordnes, 5817 Bergen, Norway [tel: +47 55 23 86 62, fax: +47 55 23 85 31, e-mail: vidarh@imr.no]

Introduction

The abundance estimate of Norwegian spring spawning herring (*Clupea harengus*) has partly been based on two acoustic winter surveys in the wintering area in Tysfjord, Ofotfjord and Vestfjord in northern Norway (Figure 1). The total biomass is calculated from the observed echo abundance, and the age structure of the population is estimated from trawl samples. These surveys have several sources for errors and uncertainties. Both the total biomass estimate and the age structure estimate may in some years suffer from the fact that the entire population is not always sampled since parts of it may select to spend the winter outside the Lofoten Islands, and not participate in the massive over-wintering in the main region. Further, the conversion to biomass from echo abundance will often be biased because of the shadowing effect (Foote et al 1992, Zhao and Ona, 2003), depth dependent target strength (Ona, 2003) and vessel avoidance (Vabø et al 2002), if these effects are not corrected for. The calculation of the respective correction factors involves uncertainty, and Aldrin et al (2006) estimate the relative contribution of the various sources of uncertainty to the uncertainty in the corrected total abundance estimate. In this paper we focus in more detail on the problem of correcting for vessel induced behaviour.

The Norwegian spring spawning herring are mainly distributed at depths between 50 and 400 m, and, especially in the upper parts of the water column, a marked avoidance behaviour has been observed in several experiments. One of these was performed in 1996, and is described in Vabø et al (2002), where the vessel avoidance is quantified by means of the vessel avoidance coefficient (VAC), defined as $s_{A,pass}/s_{A,ref}$, where $s_{A,pass}$ is the echo abundance (m^2/n.mi.^{2}) measured during vessel passage, and $s_{A,ref}$ the echo abundance averaged over a period before passage. The measured VAC was less than 0.15 in several cases for herring layers shallower than 90 m.

In Vabø et al (2002) the mean and standard deviation of the VAC are given for various depth layers for various groups of experiments. For correcting the echo abundance in a given depth layer one would like to multiply the observed echo abundance in that depth layer with a correction factor (VAC) for the actual depth layer, but the uncertainty in the estimation of the VAC should be taken into account. If the fixed mean VAC was used, the uncertainty in the final abundance estimate would be too low. Since the distribution of VAC is skewed (in Vabø et al 2002 the standard deviation is higher than the mean in some cases), it cannot be properly described by the mean and standard deviation alone, and hence these results cannot be used directly for correction purposes. In this paper an alternative approach using generalized linear models is presented.

Correcting the echo abundance in each depth layer separately is often problematic because the fish may dive before the vessel passes. An alternative approach is to correct the total echo abundance. A method for doing this based on the mean depth of the herring at the time of vessel passage is therefore also presented in this paper.

Materials and methods

Data and experimental setup

We have used data from vessel avoidance investigations carried out in 1996 and 2002-2004. An overview is given in Figure 1 and Table 1. Three different experimental setups were used in the investigations. The 1996 experiment was carried out by placing a smaller vessel

equipped with a Simrad EK500 38khz echo sounder in the path of the surveying vessel. This setup is described in detail in Vabø et al (2002). The Bergen Acoustic Buoy (BAB) was used for the 2002 and 2003 experiments. This is a free-floating buoy equipped with a Simrad EK60 38kHz echo sounder (Godø et al 1999, Godø and Totland 1999). The method has been successfully used for similar investigations (Handegard et al 2003, Jørgensen et al 2004, Handegard and Tjøstheim 2005, Skaret et al 2005, Skaret et al 2006; see these references for a more detailed description). The 2004 experiments were carried out using a lander equipped with a similar echo sounder. In this case the sounder was pinging upwards towards the surface. The depths at which the transducer was placed for the different experiments are given in Table 1.

Methods

The Vabø method

In Vabø et al (2002), the vessel avoidance coefficient at depth *d* for a given experiment *i* is calculated as

$$\mathrm{VAC}_{d,i} = \frac{s_{A,pass}^{d,i}}{s_{A,ref}^{d,i}}$$

where $s_{A,pass}^{d,i}$ is the $s_{A,}$ (area backscattering coefficient), at depth *d* for experiment *i* averaged over a 7 second interval at passing, and $s_{A,ref}^{d,i}$ is the s_A averaged over a 70 second interval ending 88 second prior to the time of passing (assumed to measure the mean, undisturbed density of herring at this position).The weighted mean VAC at depth *d* based on *n* experiments was calculated as

$$\overline{\mathrm{VAC}}_d = \frac{\frac{1}{n}\sum_{i=1}^{n} s_{A,pass}^{d,i}}{\frac{1}{n}\sum_{i=1}^{n} s_{A,ref}^{d,i}} = \frac{\sum_{i=1}^{14} s_{A,ref}^{d,i}\mathrm{VAC}_{d,i}}{\sum_{i=1}^{14} s_{A,ref}^{d,i}} \neq \frac{1}{n}\sum_{i=1}^{n}\mathrm{VAC}_{d,i},$$

and its weighted standard error as

$$\mathrm{sd}\left(\overline{\mathrm{VAC}}_d\right) = \sqrt{\mathrm{var}\left(\overline{\mathrm{VAC}}_d\right)} = \sqrt{\frac{\sum_{i=1}^{14} s_{A,ref}^{d,i}\left(\mathrm{VAC}_{d,i} - \overline{\mathrm{VAC}}_d\right)^2}{\sum_{i=1}^{14} s_{A,ref}^{d,i}}}$$

The correction factor is the inverse of $\overline{\mathrm{VAC}}_d$, and since $\mathrm{VAC}_{d,i}$ is asymmetric ($0 < \mathrm{VAC}_{d,i} < 1$ if $s_{A,pass}^{d,i} < s_{A,ref}^{d,i}$, and $1 < \mathrm{VAC}_{d,i} < \infty$ if $s_{A,pass}^{d,i} > s_{A,ref}^{d,i}$), the distribution of the correction factor is skewed, and it cannot be described by the mean and the standard error of $\overline{\mathrm{VAC}}_d$ alone. When correcting the echo abundance for avoidance, the uncertainty of the estimated correction factor should be taken into account for obtaining a realistic uncertainty measure in the corrected abundance estimate. This can be done by a bootstrap approach where the correction factor is drawn at random from its estimated distribution. However, this distribution is not possible to estimate using the above approach, since the mean and standard error are insufficient to describe the skewed distribution. Two alternative approaches are described below.

Correcting each depth layer separately using a generalized linear model

The first approach is to model $\log\left(s_{A,ref}^{d,i}\right)$ as a function of depth and $\log\left(s_{A,pass}^{d,i}\right)$ as

$$(1) \qquad \log\left(s_{A,ref}^{d,i}\right) = a_d + b\log\left(s_{A,pass}^{d,i}\right) + \varepsilon_{d,i},$$

where a_d is the intersection with the *y*-axis for depth *d*, *b* is the common slope for all depths, and $\varepsilon_{d,i}$ is random noise. To find the predicted value $\hat{s}_{A,ref}^{d}$ corresponding to a given observed value $s_{A,pass}^{d}$ at a given depth *d*, we back-transform (1) to get

$$\hat{s}_{A,ref}^{d} = \exp(\hat{a}_d)\left(s_{A,pass}^{d}\right)^{\hat{b}}\overline{\exp(\varepsilon)},$$

where $\overline{\exp(\varepsilon)}$ is a bias correcting term. This method of bias correction is known as smearing (Duan 1983). Confidence intervals for $\hat{s}_{A,ref}^{d}$ can be found by bootstrapping or analytically by using that $\log\left(\hat{s}_{A,ref}^{d}\right)$ is unbiased and normally distributed with

$$\operatorname{var}\left\{\log\left(\hat{s}_{A,ref}^{d}\right)\right\} = \operatorname{var}\left(\hat{a}_d\right) + \operatorname{var}\left(\hat{b}\right)\log\left(s_{A,pass}^{d}\right)^2 + 2\operatorname{cov}\left(\hat{a}_d,\hat{b}\right)\log\left(s_{A,pass}^{d}\right)$$

and that

$$\operatorname{cov}\left\{\log\left(\hat{s}_{A,ref}^{d_1}\right),\log\left(\hat{s}_{A,ref}^{d_2}\right)\right\} =$$
$$\log\left(s_{A,pass}^{d_1}\right)\log\left(s_{A,pass}^{d_2}\right)\left\{\operatorname{cov}(\hat{a}_{d_1},\hat{a}_{d_2}) + \operatorname{cov}(\hat{a}_{d_1},\hat{b}) + \operatorname{cov}(\hat{a}_{d_2},\hat{b}) + \operatorname{var}(\hat{b})\right\}$$

We can now simulate a correction vector $\hat{s}_{A,ref}^{*} = \left[\hat{s}_{A,ref}^{d_1*},\hat{s}_{A,ref}^{d_2*},\ldots,\hat{s}_{A,ref}^{d_p*}\right]^T$ for the depth layers $d_1, d_2, \ldots, d_p$ as

$$\hat{s}_{A,ref}^{*} = \exp\left(X^*\right)\overline{\exp(\varepsilon)}$$

where

$$X^* = \begin{bmatrix} X^{1*} \\ X^{1*} \\ \vdots \\ X^{p*} \end{bmatrix} \sim N\left(\begin{bmatrix} \log\left(\hat{s}_{A,ref}^{d_1}\right) \\ \log\left(\hat{s}_{A,ref}^{d_2}\right) \\ \vdots \\ \log\left(\hat{s}_{A,ref}^{d_p}\right) \end{bmatrix}, \begin{bmatrix} s_1^2 & s_1s_2 & \cdots & s_1s_p \\ s_1s_2 & s_2^2 & \cdots & s_2s_p \\ \vdots & \vdots & \ddots & \vdots \\ s_1s_p & s_2s_p & \cdots & s_p^2 \end{bmatrix}\right),$$

$$s_i^2 = \operatorname{var}\left\{\log\left(\hat{s}_{A,ref}^{d_i}\right)\right\}, \text{ and } s_is_j = \operatorname{cov}\left\{\log\left(\hat{s}_{A,ref}^{d_i}\right),\log\left(\hat{s}_{A,ref}^{d_j}\right)\right\}.$$

Several modifications of (1) are possible. For example, one could model an individual slope b_d for each depth, or one could let the intercept *a* and the slope *b* have some functional dependence on depth (e.g. $a = a_0 + a_1d_i + a_2d_i^2 + a_3d_i^3$). Model (1) does not take a possible diving into account. In a situation where all of the fish are situated in one depth layer before passage and move down to the next layer during passage, the model above will fail. The

correction factor will tend to infinity for the upper layer and to zero for the lower layer. A model taking this into account could be

$$\log\left(s_{A,ref}^{d,i}\right) = a_d + b\log\left(s_{A,pass}^{d,i}\right) + c\log\left(s_{A,pass}^{d^+,i}\right) + \varepsilon_{d,i}$$

where d^+ is the depth layer below d. Several terms could be included to take several depth layers into account, but a more general approach would be to use the mean depth of the fish distribution during passing.

Correcting the total s_A using mean depth at passage in a generalized linear model

An alternative approach that handles fish migration between the depth channels is to model the vessel correction factor $\mathrm{VCF}_i = s_{A,ref}^i / s_{A,pass}^i$ as

$$(2) \qquad \log\left(\mathrm{VCF}_i\right) = \log\left(\frac{s_{A,ref}^i}{s_{A,pass}^i}\right) = a + b\bar{d}_{pass} + \varepsilon_i$$

where $s_{A,ref}^i$ and $s_{A,pass}^i$ are the s_A values integrated over the whole water column before and during passage, respectively, and $\bar{d}_{pass}$ is the mean fish depth during passage. An observed $s_{A,pass}$ value with a mean depth $\bar{d}_{pass}$, could then be corrected by multiplying $s_{A,pass}$ with

$$(3) \qquad \hat{\mathrm{VCF}}_i = \exp\left(\hat{a} + \hat{b}\bar{d}_{pass}\right)\overline{\exp(\varepsilon)}$$

Confidence intervals for $\hat{\mathrm{VCF}}_i$ can be found by bootstrapping or analytically by using that $\log\left(\hat{\mathrm{VCF}}_i\right)$ is unbiased and normally distributed with variance

$$(4) \qquad \mathrm{var}\left\{\log\left(\hat{\mathrm{VCF}}_i\right)\right\} = \mathrm{var}\left(\hat{a}\right) + \mathrm{var}\left(\hat{b}\right)\bar{d}_{pass}^2 + 2\,\mathrm{cov}\left(\hat{a},\hat{b}\right)\bar{d}_{pass}.$$

In simulations we can let

$$(5) \qquad \mathrm{VCF}^* = \exp\left(X^*\right)\overline{\exp(\varepsilon)}$$

where X^* is drawn from $N\left(\log\left(\hat{\mathrm{VCF}}_i\right), \mathrm{var}\left\{\log\left(\hat{\mathrm{VCF}}_i\right)\right\}\right)$.

Results

The echograms for most of the experiments analyzed in this paper are shown in Figure 2. Close-up echograms are shown for one passage in each experiment. The vessel-induced behavior differs strongly between the various experiments. In experiment Cn8, with a herring layer at 160 to 240 meters depth, there is no visible reaction (Fig. 2 b), whereas in experiment Cn13, for more shallow herring, there is a marked diving reaction (Fig. 2 f). However, the echo abundance at passage in Cn13 is typically not much lower than before passing.

In 1996, there was a marked reduction in echo energy at passage in the upper layers, but there was not a corresponding increase in lower layers indicating a vertical replacement of the biomass through diving (Fig. 3). In 2004 the situation was quite different with an obviously

stronger diving response, particularly for G.O. Sars (Fig. 3). Thus, it would not be a good idea to fit model (1) to the 2004 experiment, whereas for the 1996 experiment the model is well suited.

Figure 4 shows the fit of model (1) to the 1996 data, and Figure 5 shows the corresponding correction factor for each depth layer with bootstrapped 95% confidence intervals. The correction is very high in shallow water, and clearly, it would have been wrong to apply these corrections to the 2004 data in Figure 3.

The alternative approach of (2) and (3) is to correct the total s_A, letting the correction depend on the mean fish depth at passing. There is a clear trend that the avoidance decreases with increasing fish depth, but the variation is huge (Fig. 6). The R-squared is only 0.25. The 2004 experiment is quite untypical with almost no reduction in echo energy even though the mean depth is small. Back-transforming the fit of Figure 6, we get a correction factor of about 4 at 50 m depth, decreasing to 1 at 300 m depth (Fig. 7).

The periods used in the analysis for averaging the reference- and passing densities $s_{A,ref}$ and $s_{A,pass}$ were chosen as in Vabø et al (2002). To check the effect of changing these periods, we averaged the reference density over the 70-second interval ending 158 seconds before passing, and the passage density over the 3-second interval starting 1 second before passing, and the results were quite similar (Fig. 8) (the 1996 experiment was not included since data for the new reference period were not available for this experiment).

Discussion

Two methods for correcting the observed echo abundance for avoidance have been presented. In the first method the correction is done at each depth layer separately, in the second the total echo abundance is corrected based on the mean depth of the fish during passing. The first method assumes that no vertical replacement of the fish takes place during vessel passage, whereas no such assumption is needed for the second method.

If the assumption of no vertical replacement is fulfilled, the first method makes it possible to estimate the vertical distribution of echo energy as it was before vessel passage, not only the total echo energy as is the case for the second method. The first method also gives us more data points to analyze than the second (one per depth layer per experiment versus one per experiment), but on the other hand the number of parameters to estimate is higher (slope and one intercept per depth layer versus slope and one intercept).

If the assumption of no vertical replacement is not fulfilled – which is often the case – the first method may lead to erroneous corrections, whereas the second method is much more robust. Still, the decrease in total echo abundance at passage may be different in two situations where the mean depth is the same. For example it may well be that the reaction will be stronger in a layer reaching from 20 to 180 m depth than in one concentrated between 90 and 110 m since the reaction in the upper parts of the first layer may be strong, and propagating downwards through the layer.

The observed variability between seasons (or experiments) is quite high. The causal factors may be recent fishing activity or predation pressure from killer whales, saithe and others. In principle, it may also occur that fish disappear from the echo beam of the stationary echo sounder because the fish is attracted towards the vessel when it approaches. This kind of behavior has been observed in many other situations (Røstad et al 2006), but the echograms and – for the 2004 experiment – measurements of the swimming velocity shows that this was not the case for the 2002-2004 experiments. However, if the small vessel carrying the

stationary transducer in the 1996 experiment was acting as a fish-attracting device (FAD), this may explain the stronger reaction observed in this experiment. Anyway, assuming no such FAD effect, the between season variability is of major concern, as it results in less accurate corrections. In fact, it makes the simulation approach in (4) and (5) a bit dubious. If the "true" avoidance for a given mean depth was constant over time and independent of location, the precision in its estimate would increase with the number of observations available, and the variation in X* in (5) would become small as the uncertainty in the parameter estimates in (4) would become small if it was based on many observations. However, if the "true" avoidance – which is unknown in a given situation where correction is needed (e.g. a survey) – varies from situation to situation, this variation should also have been reflected in the uncertainty of X* in (5). It would then be wrong to simulate X* with a very low uncertainty. In a sense, the uncertainty of (X*) is more related to the confidence intervals in Figure 6 in the case of a constant "true" avoidance, whereas it is more related to the prediction intervals in the case of a variable "true" avoidance. This is because no matter how many observations the regression is based on, the "true" avoidance in a given survey situation is unknown, and the uncertainty in the correction factor will not decrease with the number of observations/experiments on which its estimate is based.

So how should the effect of vessel induced fish behavior on abundance estimates be handled in the future? Advanced equipment for measuring the actual, undisturbed density of pelagic fish at a distance from the surveying vessel seems to be needed if absolute abundance estimates of herring close to the surface are to be achieved.

The only available now-option is to correct the measured echo energy for vessel induced effects. This can be done using eq. (2), but because of the large variation between experiments, the model should be fitted to experiments performed on each survey to obtain parameter estimates with a reasonable uncertainty. Not correcting for this effect at all may lead to serious underestimates of abundance. For other survey areas, where the herring are found in dense schools close to the surface, similar situations have been reported by comparing sonar observations with measured density by the research vessel echo sounder (Misund et al 1996, Soria et al 1996). Similar correction factors as observed here for the echo sounder estimate was needed to achieve the sonar abundance for herring, while a non-reactive species like pilchard gave similar estimates in the two systems (Misund et al 1996).

Acknowledgements

We are grateful to the Norwegian Research Council for financial support.

Without the effort from senior engineers Ingvald Svellingen, Terje Torkelsen, Atle Totland and Ronald Pedersen these experiments could not have been performed. We were also dependent of the seamanship of the skipper and crew on RV Johan Hjort and RV G.O. Sars.

References

Aldrin, M., Løland, A., and Ona, E. 2006. Estimating and decomposing total uncertainty for survey-based abundance estimates of Norwegian spring-spawning herring. ICES CM 2006/I:13.

Duan, N. 1983. Smearing estimate - a nonparametric retransformation method. Journal of the American Statistical Association, 78: 605-610.

Foote, K.G., Ona, E. & Toresen, R. 1992. Determining the extinction cross section of aggregating fish. J. Acoust Soc. Am. 91(4,1), 1983-1989.

Godø, O.R., and Totland, A. 1999. Bergen acoustic buoy (BAB) - a tool for remote monitoring marine resources. Joint IASA/EASA meeting Berlin. Paper 2pAO10.

Godø, O.R., Somerton, D., and Totland, A. 1999. Fish behaviour during sampling as observed from free floating buoys - application for bottom trawl survey assessment. ICES CM/J:10.

Handegard, N.O., Michalsen, K., and Tjøstheim, D. 2003. Avoidance behaviour in cod (*Gadus morhua*) to a bottom-trawling vessel. Aquatic Living Resources, 16: 265-270.

Handegard, N.O., and Tjøstheim, D. 2005. When fish meets a trawling vessel: examining the behaviour of gadoids using a free floating buoy and acoustic split-beam tracking. Canadian Journal of Fisheries and Aquatic Sciences, 62: 2409-2422.

Jørgensen, R., Handegard, N.O., Gjøsæter, H., and Slotte, A. 2004. Possible vessel avoidance behaviour of capelin in a feeding area and on a spawning ground. Fisheries Research, 69: 251-261.

Misund, O.A., Aglen, A., Hamre, J., Ona, E. Røttingen, I, Skagen, D, and Valdemarsen, J.W. 1996. Improved mapping of schooling fish near surface: comparison of abundance estimates obtained by sonar and echo integration. ICES J. Mar. Sci, 53, 383 –388.

Ona, E. 2003. An expanded target-strength relationship for herring. – ICES Journal of Marine Science, 60: 493–499.

Røstad, A., Kaartvedt, S., Klevjer, T. A., and Melle, W. 2006. Fish are attracted to vessels. ICES Journal of Marine Science, In press.

Skaret, G., Slotte, A., Handegard, N.O., Axelsen, B.-E., and Jørgensen, R. 2006. Pre-spawning herring in a protected area showed only moderate reaction to a surveying vessel. Fisheries Research, 78: 359-367.

Skaret, G., Axelsen, B.-E., Nøttestad, L., Fernö, A., and Johannessen, A. 2005. The behaviour of spawning herring in relation to a survey vessel. ICES Journal of Marine Science, 62: 1061-1064.

Soria, M., Fréon, P., and Gerlotto, F. 1996. Analysis of vessel influence on spatial behaviour of fish schools using a multi-beam sonar and consequences for biomass estimates by echo-sounder. ICES Journal of Marine Science, 53: 453-458.

Vabø, R., Olsen, K., and Huse, I. 2002. The effect of vessel avoidance of wintering Norwegian spring spawning herring. Fisheries research, 58: 59-77.

Zhao, X., and Ona, E. 2003. Estimation and compensation models for the shadowing effect in dense fish aggregations. ICES Journal of Marine Science, 60: 155–163.

Table 1. Overview of experiments.

Cruise (Cn)	Exp (En)	Year	Start time	Stop time	Passages	Bottom depth	Trans. depth	Vessel	Platform
		1996	16. Dec 10:00	17. Dec 21:00	34	130-720	12	JH	Vessel
7	1	2001	21. Jan 20:00	22. Jan 11:45	11	600	35	Sarsen	BAB
8	2	2002	11. Jan 08:15	11. Jan 08:15	6	370-420	20	JH	BAB
13	1	2003	2. Dec 14:33	3. Dec 07:28	13	100-220	10	GOS/JH	BAB
13	2	2003	4. Dec 20:40	5. Dec 08:38	10	480-550	10	GOS/JH	BAB
13	3	2003	5. Dec 17:05	6. Dec 08:14	19	220-550	10	GOS/JH	BAB
13	4	2003	8. Dec 19:15	8. Dec 22:18	2	450-550	10	GOS/JH	BAB
13	6	2003	12. Dec 00:10	12. Dec 03:41	4	550	10	GOS/JH	BAB
14	2	2004	3. Dec 22:59	4. Dec 17:53	11	137	137	GOS/JH	Lander

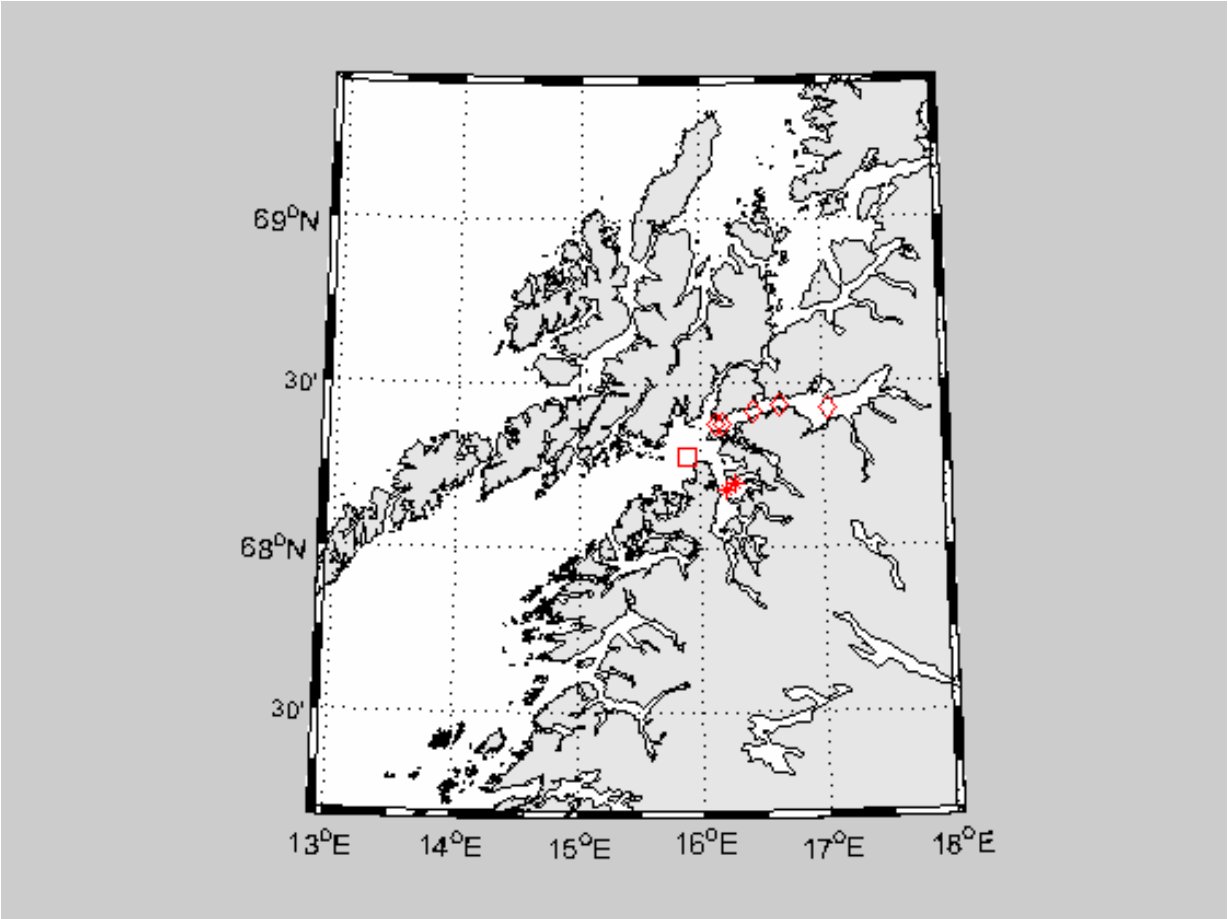

Figure 1. Overview of experimental locations. Square, asterisk and diamond denotes the experiments in 2001, 2002 and 2003, respectively, using the BAB method. Plus sign denotes the experiment in 1996 using the smaller boat and x denotes the lander experiments in 2004. (+ anx x to be added).

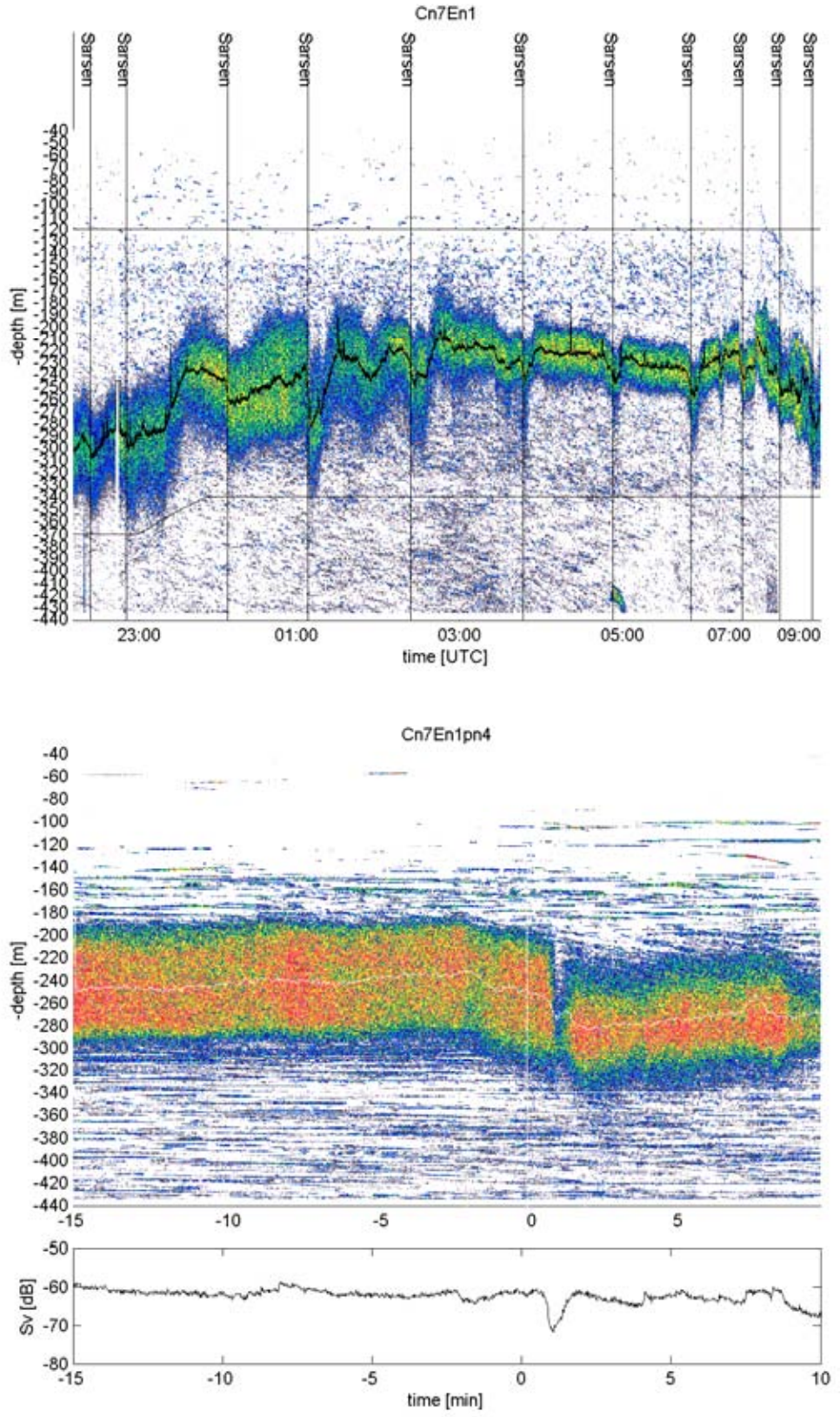

Figure 2a. Top: echogram for cruise Cn7 (21. des. 2001). Vertical lines indicate passage. The thick black curve indicates mean depth. Only data between the thin horizontal lines were used. The vessel is the old G.O. Sars (Sarsen). Bottom: close-up of passage No. 4.

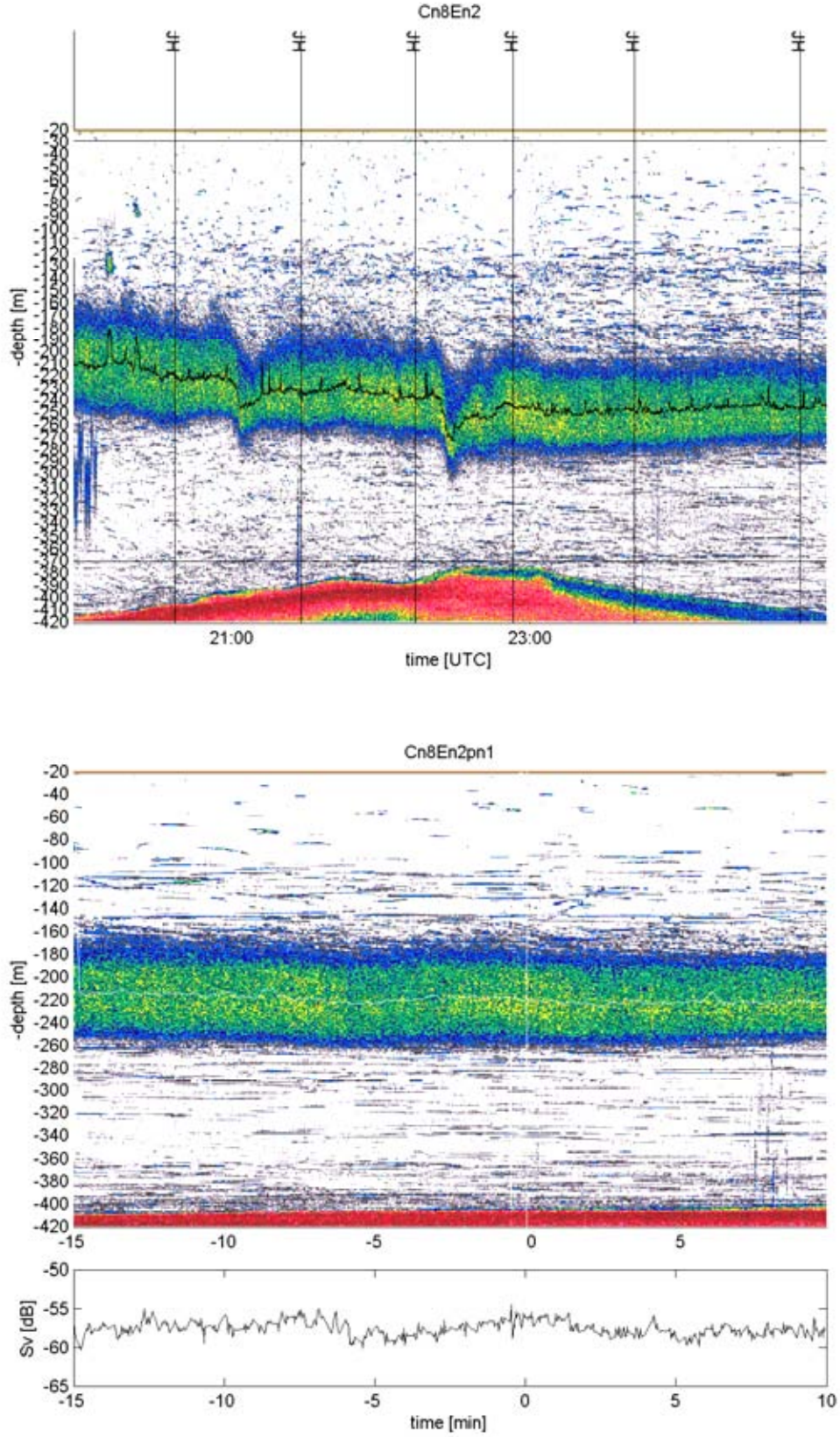

Figure 2b. Top: echogram for cruise Cn8 (11. Jan. 2002). Vertical lines indicate passage. The thick black curve indicates mean depth. Only data between the thin horizontal lines were used. The vessel is Johan Hjort. Bottom: close-up of passage No. 1.

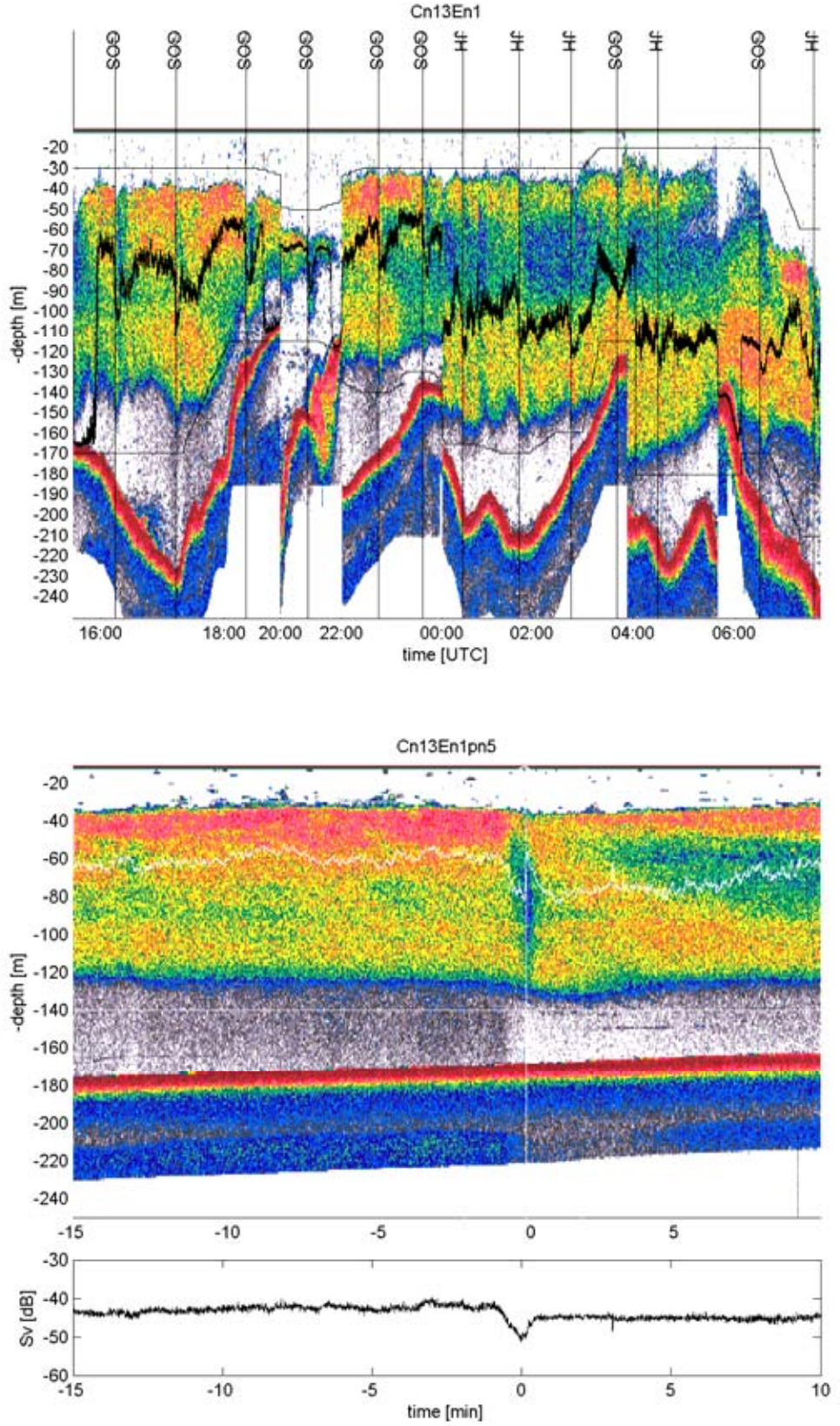

Figure 2c. Echograms for cruise Cn13, experiment En1 (2-3. des. 2003). Vertical lines indicate passage. The thick black curve indicates mean depth. Only data between the thin horizontal curves were used. The vessels are the new G.O. Sars (GOS), and Johan Hjort (JH). Bottom: close-up of passage no 5.

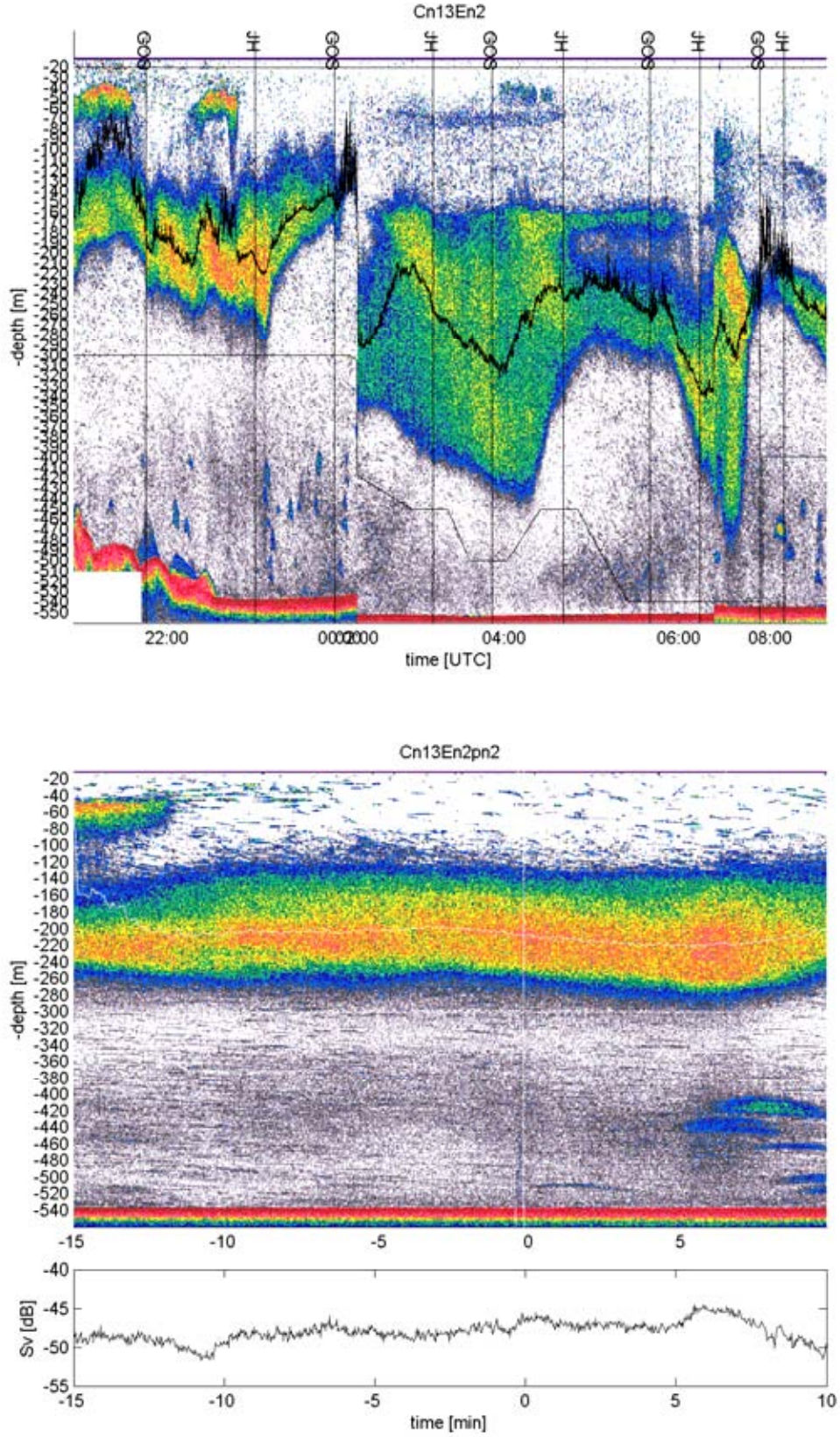

Figure 2c. Echograms for cruise Cn13, experiment En2 (4-5. des. 2003). Vertical lines indicate passage. The thick black curve indicates mean depth. Only data between the thin horizontal curves were used. The vessels are the new G.O. Sars (GOS), and Johan Hjort (JH). Bottom: close-up of passage no 2.

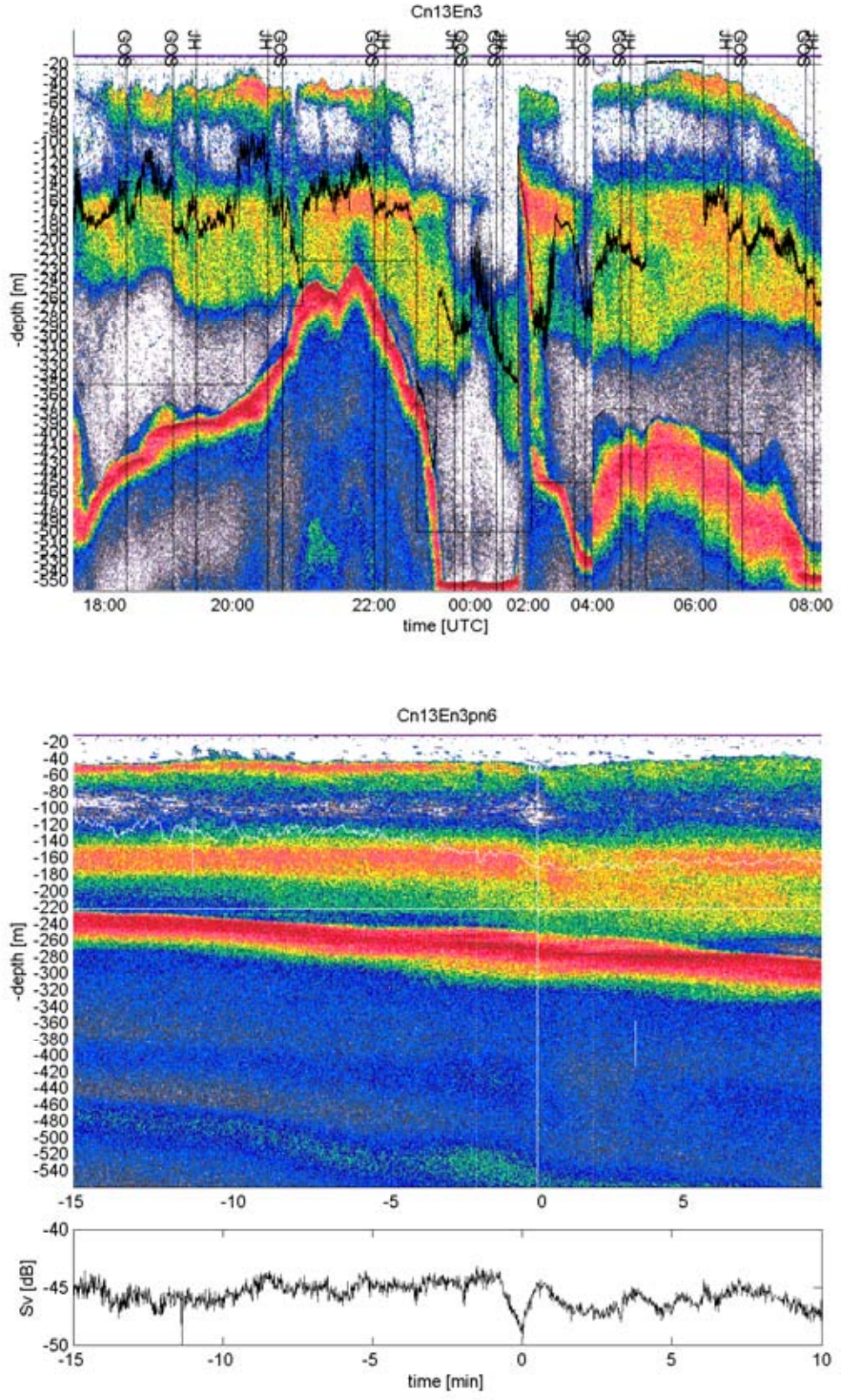

Figure 2d. Echograms for cruise Cn13, experiment En3 (5-6. des 2003). Vertical lines indicate passage. The thick black curve indicates mean depth. Only data between the thin horizontal curves were used. The vessels are the new G.O. Sars (GOS), and Johan Hjort (JH). Where two passages occur with less than 30 min interval, only the first of these is used. Bottom: close-up of passage no. 6.

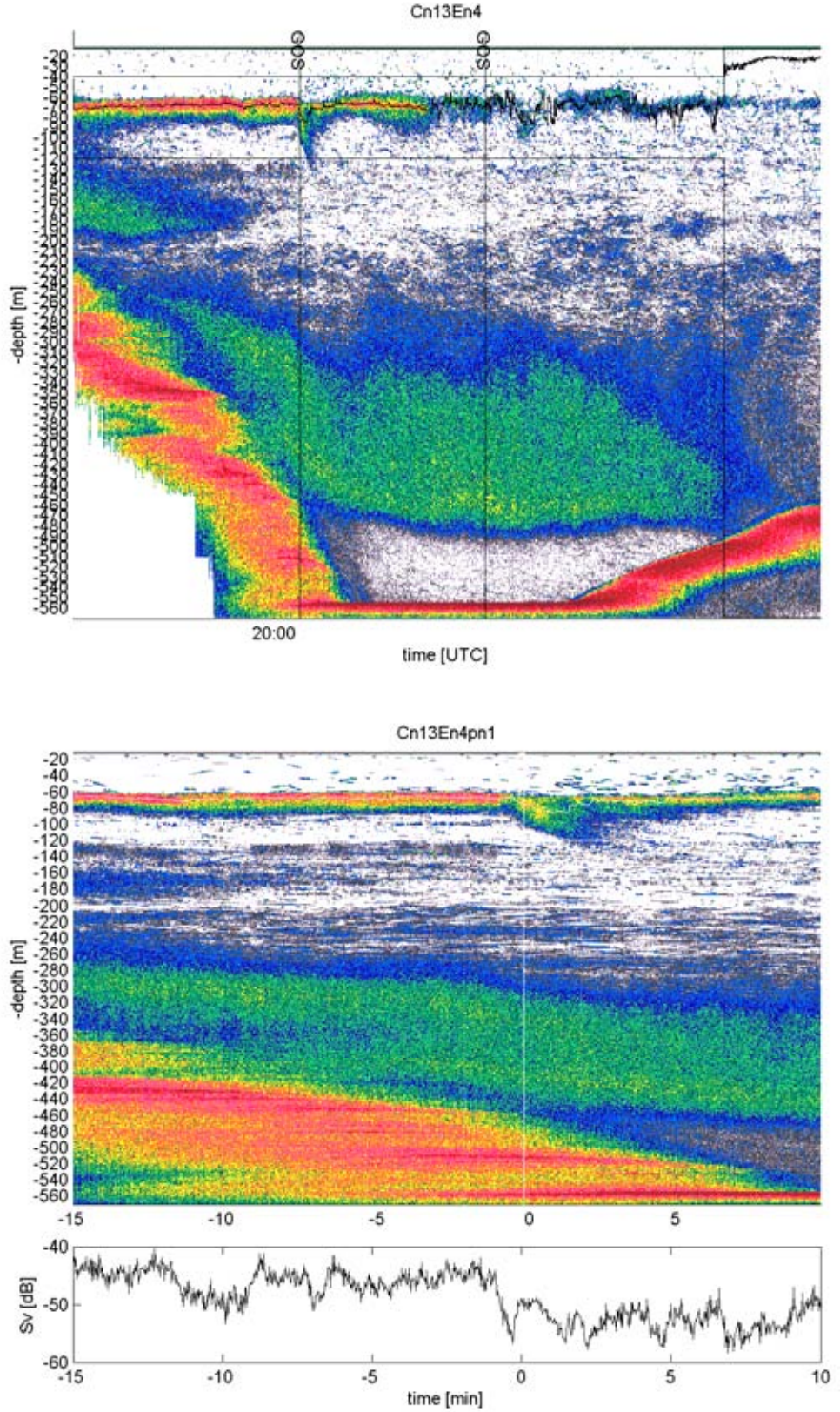

Figure 2e. Echograms for cruise Cn13, experiment En4 (8. des 2003). Vertical lines indicate passage. The thick black curve indicates mean depth. Only data between the thin horizontal curves were used. The vessel is the new G.O. Sars (GOS). Bottom: close-up of passage no. 1.

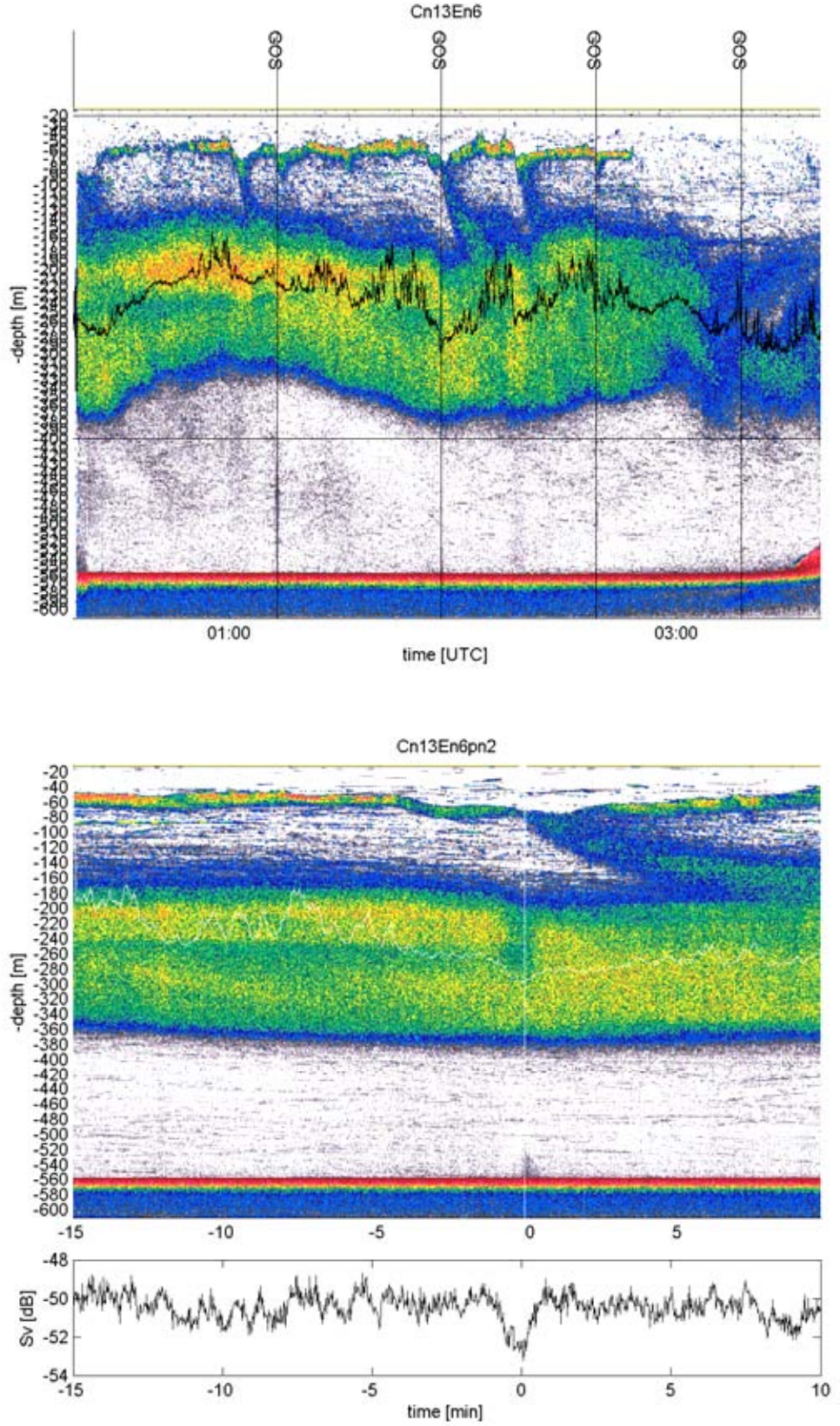

Figure 2f. Echograms for cruise Cn13, experiment En6 (12. des. 2003). Vertical lines indicate passage. The thick black curve indicates mean depth. Only data between the thin horizontal curves were used. The vessel is the new G.O. Sars (GOS). Bottom: close-up of passage no. 2.

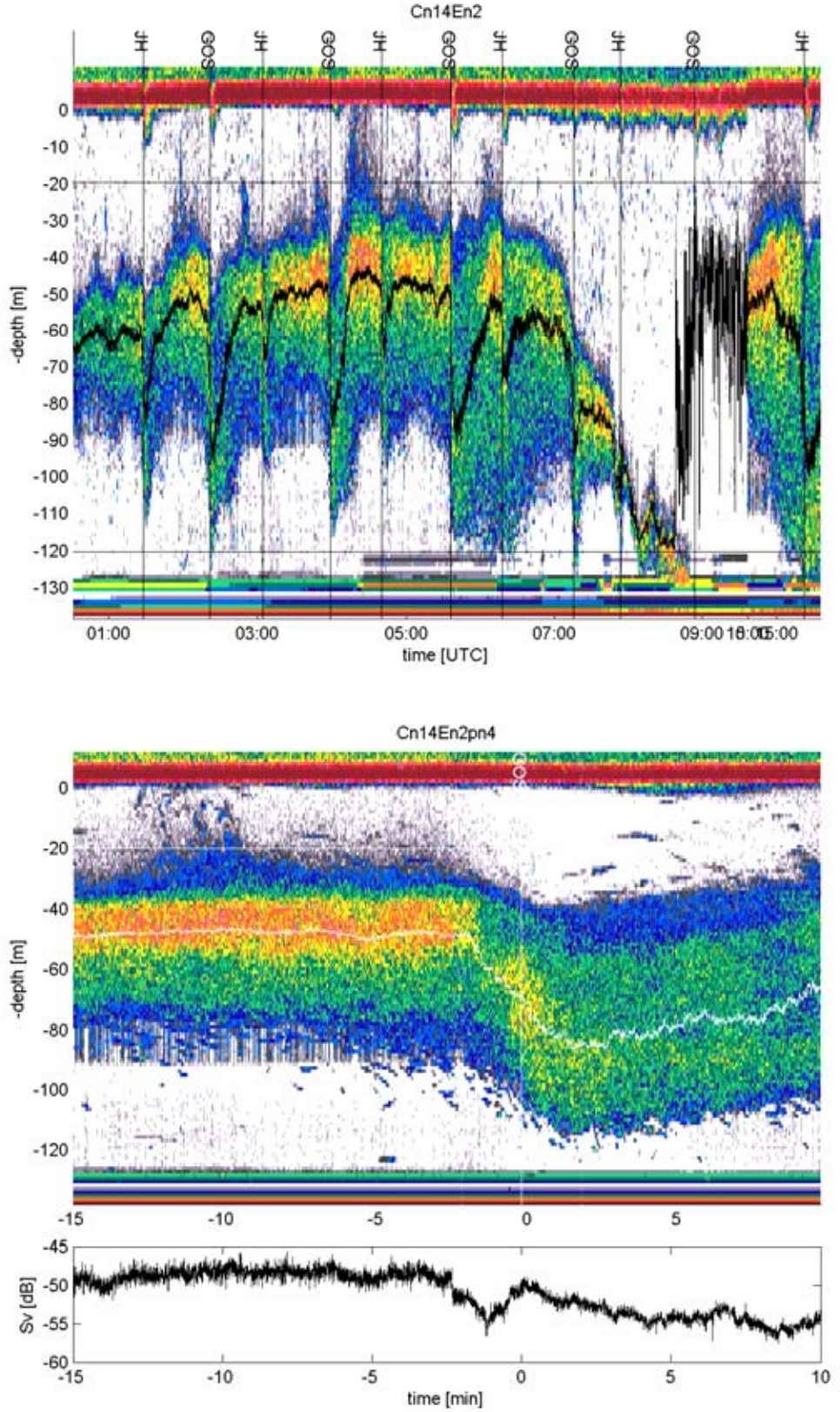

Figure 2g. Echograms for cruise Cn14, experiment 2 (3. des. 2004). Vertical lines indicate passage. The thick black curve indicates mean depth. Only data between the thin horizontal lines were used. The vessels are the new G.O. Sars (GOS), and Johan Hjort (JH). The last passage of G.O. Sars was not used. Bottom: close-up of passage no. 4.

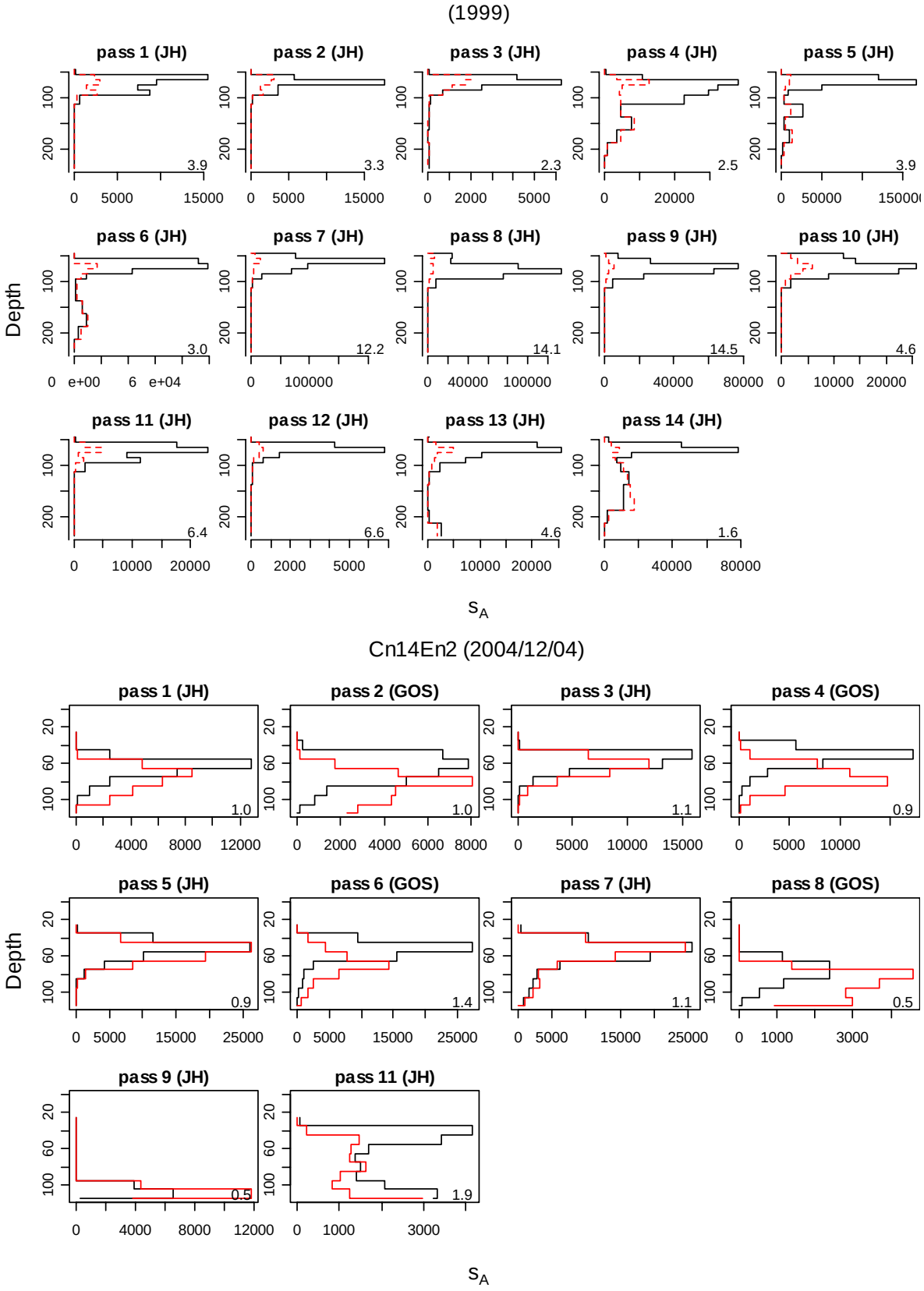

Figure 3. Vertical density profiles before passage (black) and during passage (red) for some of the passages of the 1996 (top) and 2004 (bottom) experiment. The vessels are Johan Hjort (JH) and G.O. Sars (GOS). The numbers in the lower right corners shows the ratio $s^i_{A,ref} / s^i_{A,pass}$ integrated over the whole water column.

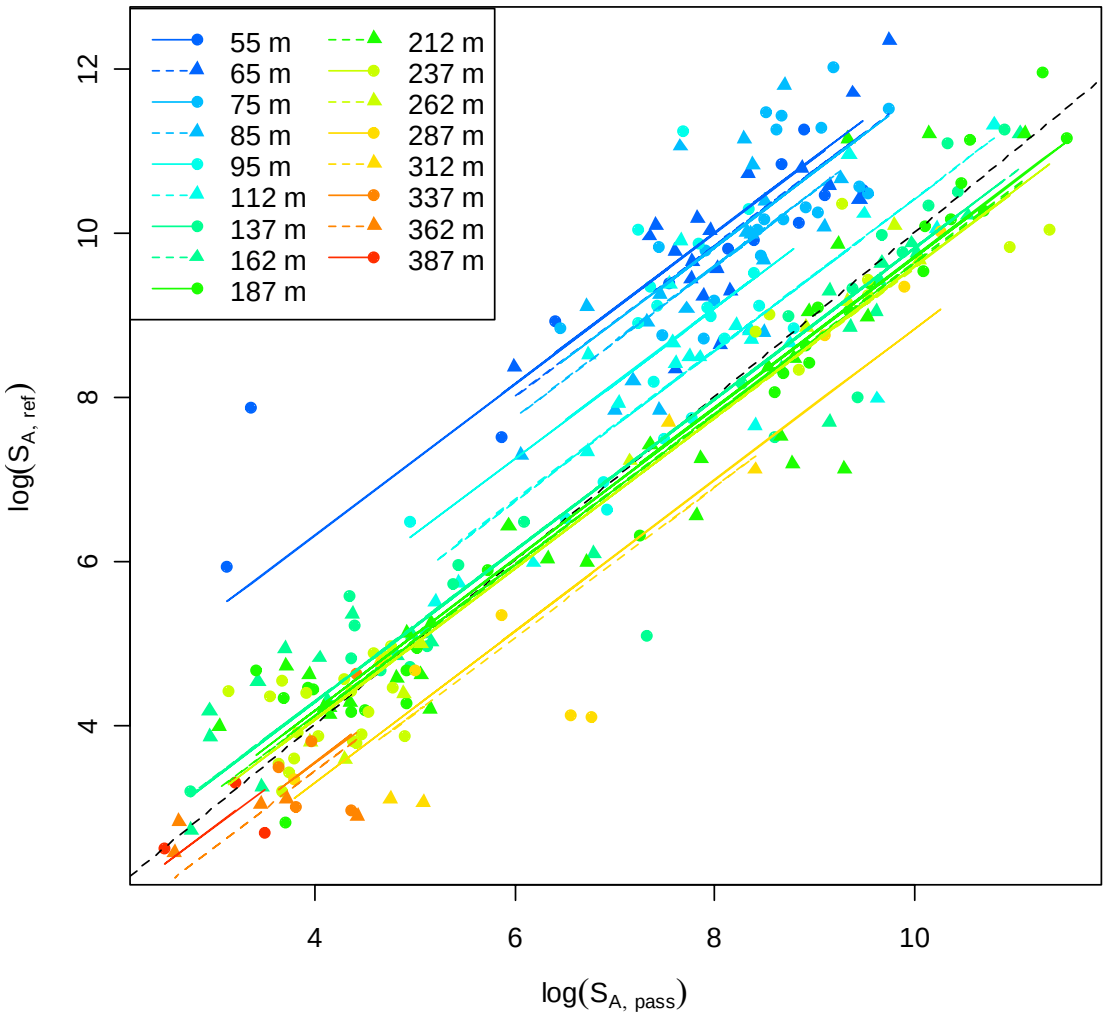

Figure 4. Points: $\log\left(s_{A,ref}^{d,i}\right)$ plotted against $\log\left(s_{A,pass}^{d,i}\right)$ for all passages in 1996 for depths > 50 m. Combinations (d,i) where $s_{A,ref}^{d,i} < 10$ or $s_{A,pass}^{d,i} < 10$ are excluded. Lines: the fit of model (1). The depths in the legend are the midpoints in the 10 and 25 m depth channels.

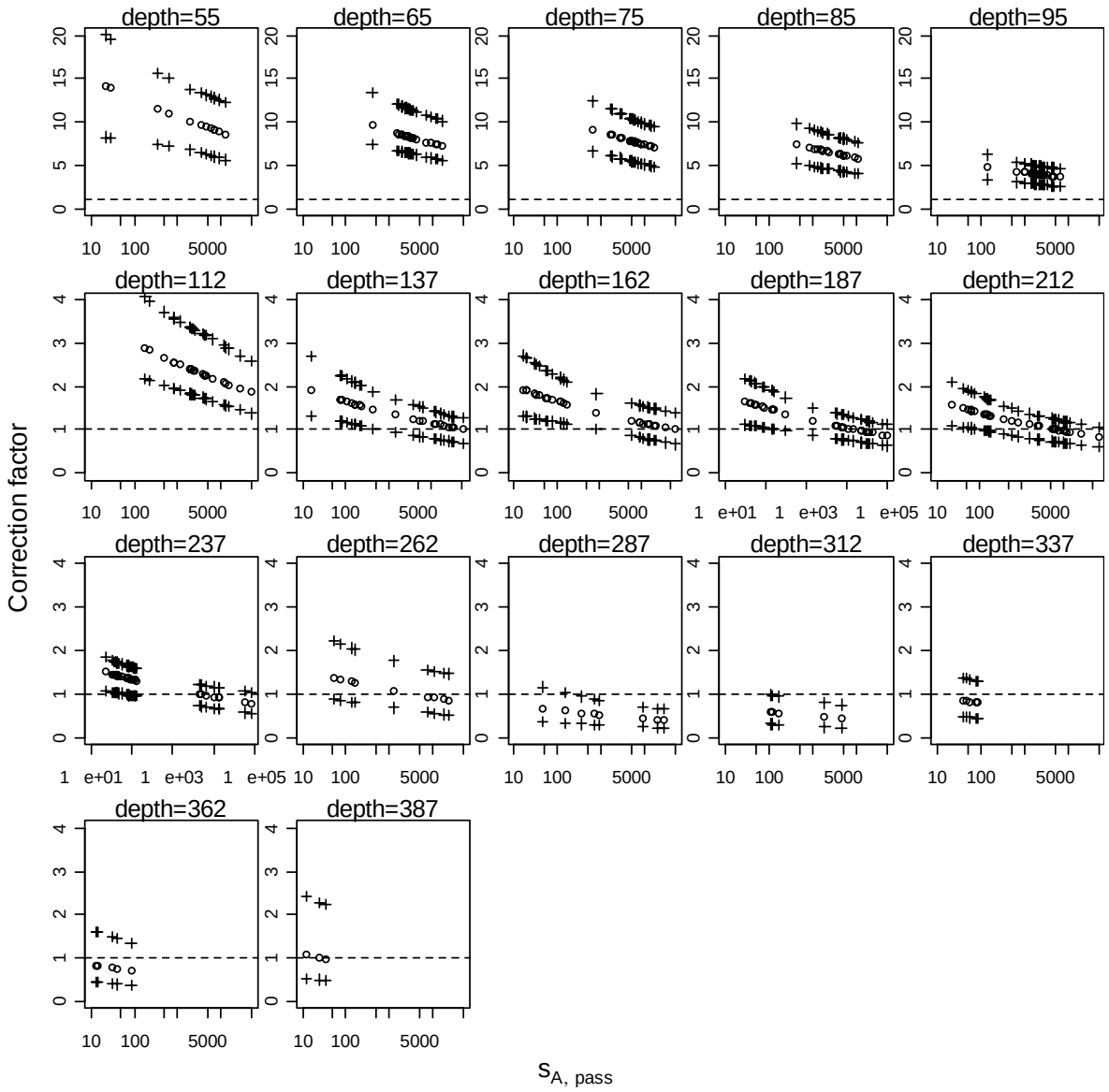

Figure 5. Correction factor $\hat{S}^d_{A,ref} / S^d_{A,pass}$ as a function of depth and $S^d_{A,pass}$ with 95% bootstrapped confidence intervals. The correction factor is calculated from the fit in Figure 4.

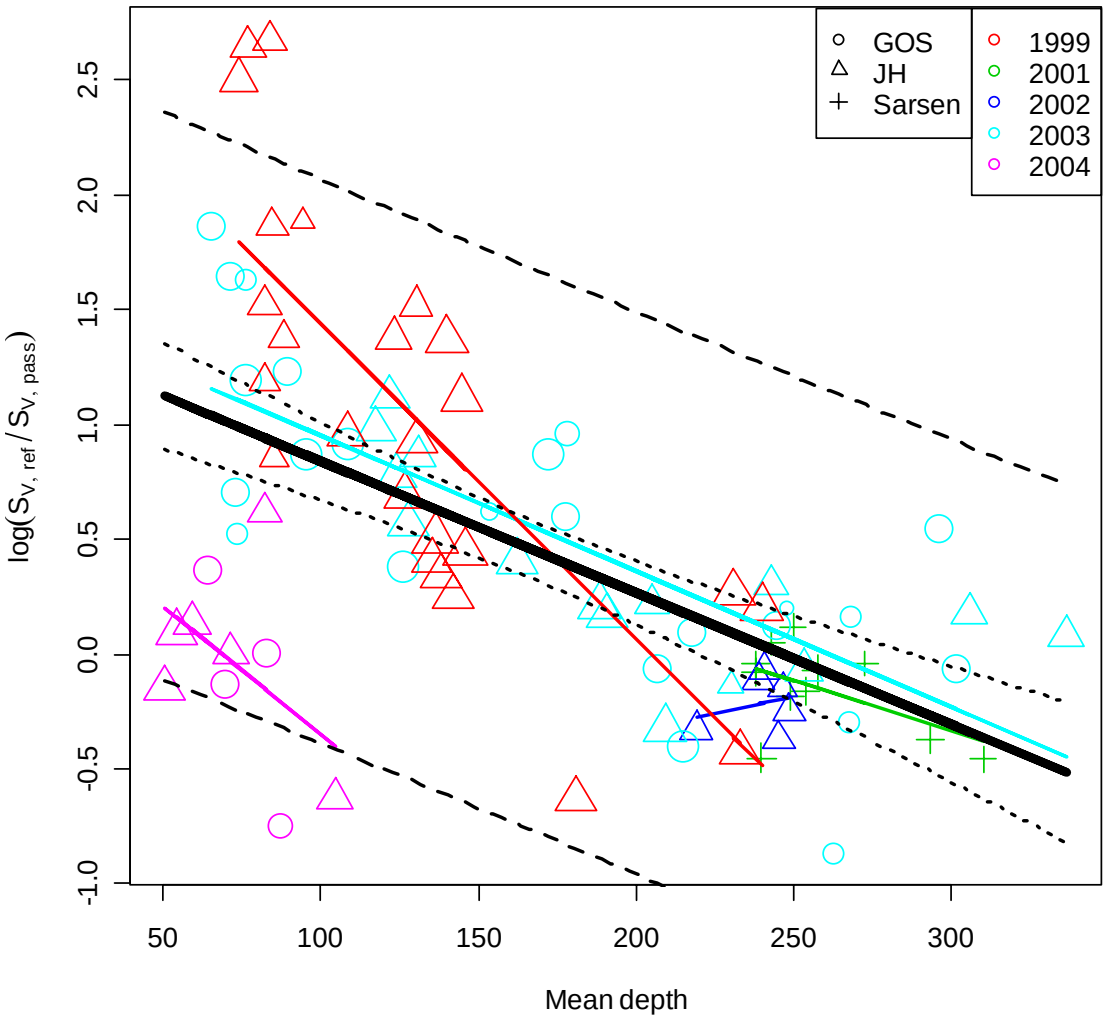

Figure 6. $\log\left(\hat{s}_{A,ref} / s_{A,pass}\right)$ as a function of mean fish depth at passage. Regression lines from model (2) are fitted to the data from each year (coloured lines) and to all of the data (thick black line). The dashed and dotted black lines show the 95% prediction and confidence intervals, respectively, calculated from all of the data. The size of the symbols is proportional to $\log\left(s_{A,pass}\right)$.

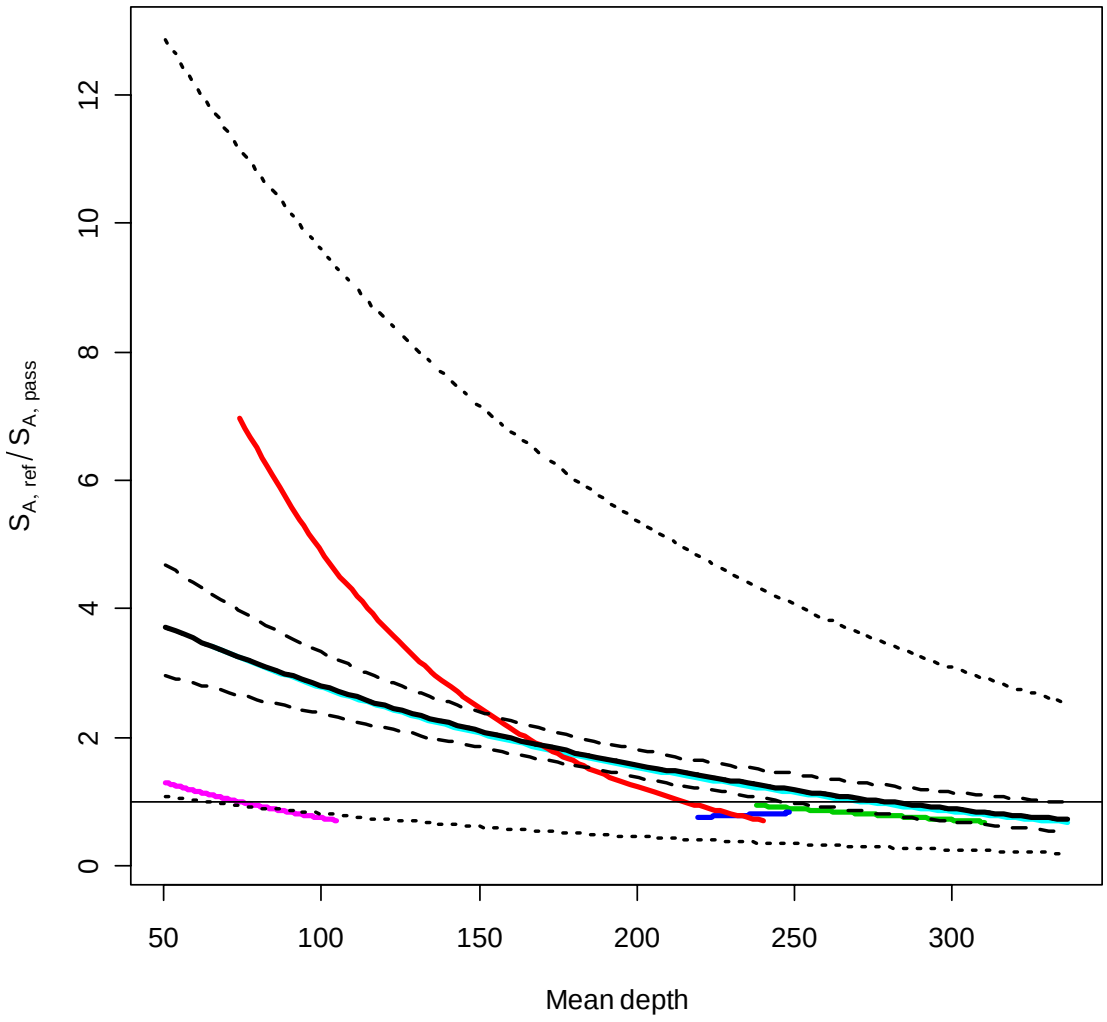

Figure 7. The fits in Figure 6 back-transformed according to (3). The dashed and dotted black lines show the bias-corrected 95% confidence and prediction intervals, respectively. The coloured lines correspond to the coloured regression lines in Figure 6. A horizontal line is drawn at $\hat{s}_{A,ref} / s_{A,pass} = 1$.

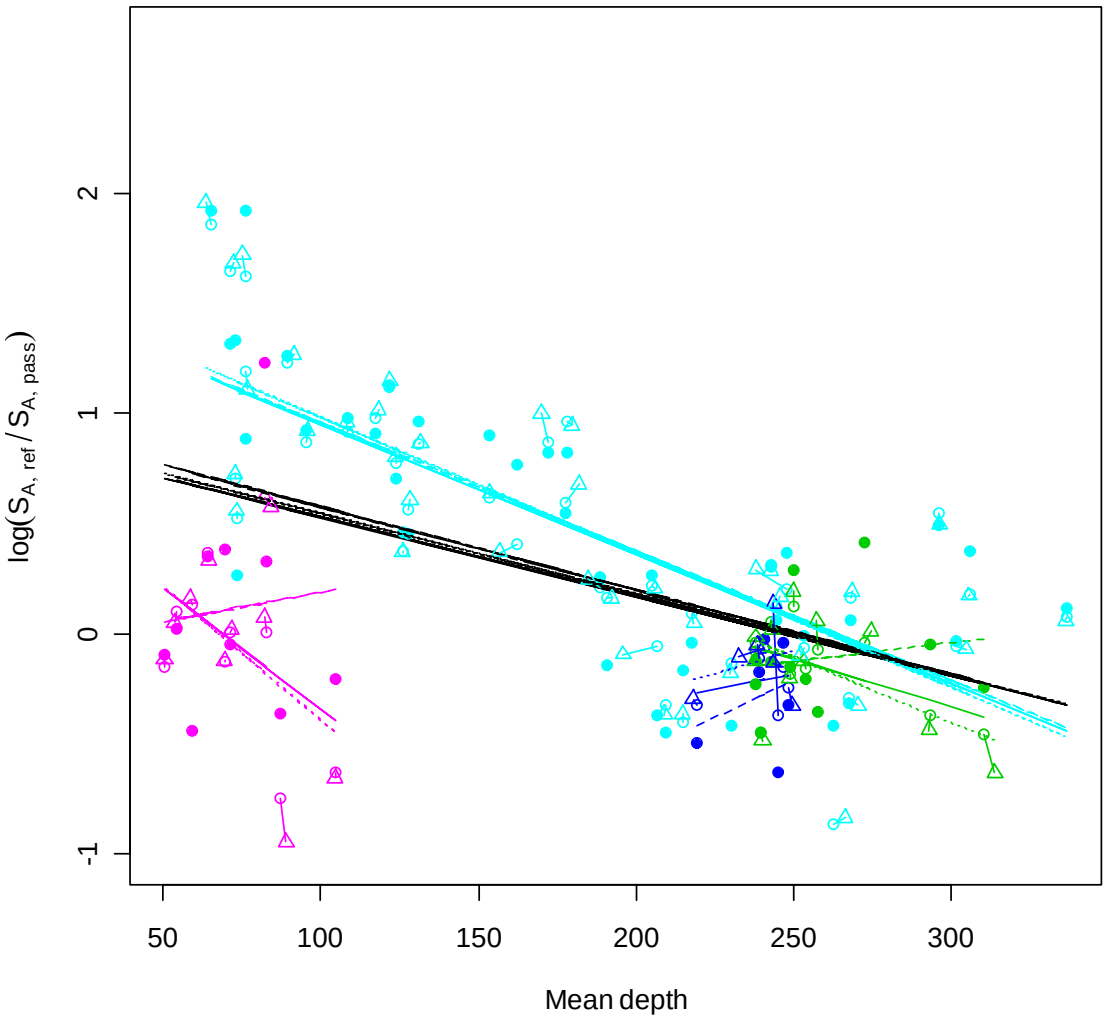

Figure 8. $\log\left(\hat{s}_{A,ref} / s_{A,pass}\right)$ as a function of mean fish depth at passage for different definitions of the time intervals over which $\hat{s}_{A,ref}$ and $s_{A,pass}$ were averaged. Regression lines from model (2) are fitted to the data from each year (coloured lines) and to all of the data (thick black line). Open circles / solid lines: reference interval 158-88 seconds before passage and passage interval 7 seconds around passing (the original intervals). Filled circles / dashed lines: reference interval 228-158 seconds before passage and passage interval 7 seconds around passing. Triangles / dotted lines: reference interval 158-88 seconds before passage and passage interval 3 seconds around passing. The open and filled circles from the same experiment have the same mean depth. The open circle and the triangle from the same experiment are connected with a line.